Triglyme−Li$^+$ Cation Solvate Structures: Models for Amorphous Concentrated Liquid and Polymer Electrolytes (I)

Wesley A. Henderson,*,[†] Neil R. Brooks,[‡] William W. Brennessel,[‡] and Victor G. Young, Jr.[‡]

Department of Chemical Engineering & Materials Science, and X-ray Crystallographic Laboratory, Department of Chemistry, University of Minnesota, Minneapolis, Minnesota 55455

Received May 13, 2003

Crystalline phases of (triglyme)$_1$:LiX (X = $CF_3SO_3^-$, BF_4^-, ClO_4^-, and AsF_6^-) have been isolated and structurally characterized. The phases are isostructural and represent a novel form of Li$^+$ cation coordination not observed in crystalline poly(ethylene oxide) (PEO)−salt phases. The crystal structure of a (triglyme)$_1$:LiBPh$_4$ phase has also been determined, which differs markedly from those found with the smaller anions. In addition, a more concentrated (triglyme)$_{2/3}$:LiCF$_3$SO$_3$ phase has been characterized, which also displays a novel form of Li$^+$ cation coordination. Such solvates represent models for interchain cation transport transition states in concentrated liquid and amorphous PEO electrolytes.

Introduction

Extensive research efforts have been devoted to the development of concentrated liquid and solid polymer electrolytes for use in electrochemical devices such as lithium batteries.[1−5] This development has been hindered, however, by the relatively poor understanding of how ions are transported through the electrolytes. Poly(ethylene oxide), PEO, is the archetype of ionically coordinating polymers used as solid solvents.[1] Solid electrolytes prepared from PEO and polymers containing ethoxy segments have some of the highest ionic conductivities reported and thus have received the most attention for solid polymer electrolyte applications.

The ionic conductivity is typically highest for fully amorphous electrolytes. It is therefore desirable to investigate the nature of solvate structures in amorphous phases to better understand the ionic conductivity mechanisms in concentrated electrolytes. Insight into such structures may be obtained from the structures of crystalline phases. Bruce's research group has extensively explored the crystal structures of PEO−salt phases for this purpose.[6,7] Although much information has been gleaned in this way, packing constraints and the long-range ordering of the polymeric chains limit the number of solvate structures which may form.

In the amorphous phase, however, the absence of these restrictions permits other localized solvate structures to form preferentially. Many more solvate structures may therefore form in amorphous PEO−LiX mixtures which cannot be observed through PEO−LiX crystal structure determination. The small size of the Li$^+$ cations, however, restricts the number of solvent donor atoms and/or anions which may coordinate a given cation (enter the cation's primary solvation sphere) at one time to form a solvate structure. Li$^+$ cation coordination numbers from 3 to 8 have been found, but 3-fold coordination is very rare as is 7- or 8-fold coordination.[8] Typically, coordination numbers of 4−6 are found in crystalline solvates as well as in amorphous PEO−LiX mixtures.[9−11] The solvate structures formed may be stable or transient in nature. But the number of ways in which one or more chains of ether oxygens (EOs) and anions may coordinate a Li$^+$ cation is limited (even in amorphous mixtures). Glyme−LiX crystalline solvate structures provide direct information regarding both how this coordination occurs as well as the influence of the EO/Li concentration, temperature, and anions upon the solvate formation.

The coordination found in the crystalline solvates may not represent all of the possible localized Li$^+$ cation solvate states which exist in amorphous materials. This is especially true at higher temperatures where higher energy, less favorable amorphous solvates may form. But the crystalline solvates show what is possible (they are true low-energy states) and, when combined with molecular models and vibrational spectroscopy, they provide a great deal of information for clarifying ionic

---

* To whom correspondence should be addressed. E-mail: wesley.henderson@casaccia.enea.it.

[†] Department of Chemical Engineering & Materials Science.

[‡] X-ray Crystallographic Laboratory, Department of Chemistry.

(1) Gray, F. M. *Solid Polymer Electrolytes: Fundamentals and Technological Applications*; VCH Publ., Inc.: New York, 1991.

(2) MacCallum, J. R., Vincent, C. A., Eds. *Polymer Electrolyte Reviews-1*; Elsevier Applied Science Publ., Ltd: New York, 1987.

(3) MacCallum, J. R., Vincent, C. A., Eds. *Polymer Electrolyte Reviews-2*; Elsevier Applied Science Publ., Ltd: New York, 1989.

(4) Gray, F. M. *Polymer Electrolytes*; The Royal Society of Chemistry: Cambridge, UK, 1997.

(5) Bruce, P. G., Ed. *Solid State Electrochemistry*; Cambridge University Press: New York, 1995.

(6) Andreev, T. G.; Bruce, P. G. *Electrochim. Acta* **2000**, *45*, 1417.

(7) Andreev, T. G.; Bruce, P. G. *J. Phys.: Condens. Matter* **2001**, *13*, 8245.

(8) Olsher, U.; Izatt, R. M.; Bradshaw, J. S.; Dalley, N. K. *Chem. Rev.* **1991**, *91*, 137.

(9) Londono, J. D.; Annis, B. K.; Habenschuss, A.; Brodin, O.; Smith, G. D.; Turner, J. Z.; Soper, A. K. *Macromolecules* **1997**, *30*, 7151.

(10) Mao, G.; Saboungi, M.-L.; Price, D. L.; Armand, M. B.; Howells, W. S. *Phys. Rev. Lett.* **2000**, *84*, 5536.

(11) Mao, G.; Saboungi, M.-L.; Price, D. L.; Badyal, Y. S.; Fischer, H. E. *Europhys. Lett.* **2001**, *54*, 347.

10.1021/cm034351z CCC: $25.00

transport mechanisms in concentrated electrolyte mixtures. For this reason, a comprehensive study of the structures and phase behavior of glyme, $CH_3O-(CH_2CH_2O)_n-CH_3$ ($n = 1-4$), crystalline solvates with lithium salts has been undertaken. The solvates formed between lithium salts and triglyme are reported here, which suggest two possible mechanisms for Li^+ cation transport between PEO chains. This work complements molecular modeling studies of G3$-Li^+$ cation interactions.[12-15] Triglyme ($n = 3$) is denoted as G3 after the notation used by other authors.[16,17]

Experimental Section

Materials. Preparation and storage of the reagents and single crystals were performed in a dry room (<1% relative humidity, 22 °C). G3 (triglyme or tri(ethylene glycol) dimethyl ether) (Aldrich) was dried over 4-Å molecular sieves and used without further purification. $LiCF_3SO_3$, $LiClO_4$, and $LiAsF_6$ (Aldrich) were dried for 24 h under high vacuum at 110, 110, and 70 °C, respectively. $LiBF_4$ (Aldrich) was purchased as anhydrous and used as-received. $LiBPh_4$ was prepared by etherate decomposition of the monoglyme solvate $(G1)_3$:$LiBPh_4$ (Aldrich). $(G1)_3$:$LiBPh_4$ was heated under vacuum at 170 °C for 5 h and then at 130 °C for 12 h to remove the G1.

Synthesis of $(G3)_1$:$LiCF_3SO_3$, $(G3)_1$:$LiClO_4$, $(G3)_1$:$LiAsF_6$, $(G3)_1$:$LiBF_4$, and $(G3)_1$:$LiBPh_4$. G3 was added to the salts—$(G3)_1$:$LiCF_3SO_3$: G3 (1.154 g, 6.47 mmol), $LiCF_3SO_3$ (0.505 g, 3.24 mmol); $(G3)_1$:$LiClO_4$: G3 (0.809 g, 4.54 mmol), $LiClO_4$ (0.161 g, 1.51 mmol); $(G3)_1$:$LiAsF_6$: G3 (0.614 g, 3.44 mmol), $LiAsF_6$ (0.471 g, 2.40 mmol); $(G3)_1$:$LiBF_4$: G3 (0.834 g, 4.68 mmol), $LiBF_4$ (0.109 g, 1.16 mmol); and $(G3)_1$:$LiBPh_4$: G3 (0.337 g, 1.89 mmol), $LiBPh_4$ (0.206 g, 0.63 mmol). The mixtures were heated while stirring to dissolve the salts. Colorless, block crystals of $(G3)_1$:$LiCF_3SO_3$ ($T_m = 40$ °C) grew on storage in a refrigerator at 5 °C for 1 week in a hermetically sealed coffee bag. Colorless, block crystals of $(G3)_1$:$LiClO_4$ ($T_m = 103$ °C), $(G3)_1$:$LiAsF_6$ ($T_m = 120$ °C), $(G3)_1$:$LiBF_4$ ($T_m = 90$ °C), and $(G3)_1$:$LiBPh_4$ grew slowly on storage in the dry room at 22 °C for several days to weeks.

Synthesis of $(G3)_{2/3}$:$LiCF_3SO_3$. G3 (0.634 g, 3.55 mmol) was added to $LiCF_3SO_3$ (0.541 g, 3.47 mmol). The mixture was heated while stirring to dissolve the salt. Block crystals of $(G3)_{2/3}$:$LiCF_3SO_3$ ($T_m = 47$ °C) grew slowly on storage in the dry room at 22 °C for several weeks. Note that although the stoichiometry of the G3:$LiCF_3SO_3$ mixture was 1:1, crystals of $(G3)_1$:$LiCF_3SO_3$ did not form. Rather, the mixture remains a clear liquid for days to weeks with crystals of $(G3)_{2/3}$:$LiCF_3SO_3$ slowly separating. This is attributed to the significant hysteresis that is typically observed in glyme−lithium salt mixtures between the crystallization and melting temperatures. In the amorphous solutions, ions may be aggregated in some cases, leading to nucleation of the more concentrated phase rather than the thermodynamically predicted one.

General Procedures. Melting temperatures were determined from the peak temperatures of heating thermograms using a Perkin-Elmer Pyris 1 differential scanning calorimeter. Samples were hermetically sealed in Al pans in the dry room. The sample pans were slowly cooled from 20 to −120 °C and then heated from −120 to 140 °C at a heating rate of 10 °C/min.

X-ray Structural Determination. Single crystals of the solvates were placed on the tip of a 0.1-mm-diameter glass capillary and mounted on a Bruker SMART system diffractometer for data collection at −100 °C. An inert atmosphere glovebag was used to prevent exposure of the crystals to moisture in the air. Data collection was carried out using Mo Kα radiation (graphite monochromator). Intensity data were corrected for absorption and decay.[18] Final cell constants were calculated from the *xyz* centroids of the strong reflections from the actual data collection after integration.[19] Structures were solved using SIR92[20] ($(G3)_1$:$LiCF_3SO_3$ and $(G3)_{2/3}$:$LiCF_3SO_3$), SIR97[21] ($(G3)_1$:$LiBF_4$ and $(G3)_1$:$LiBPh_4$), SHELXS-86[22] ($(G3)_1$:$LiAsF_6$), and SHELXS-97[22] ($(G3)_1$:$LiClO_4$) and refined using SHELXL-97.[22] Direct-methods solutions were calculated, which provided most non-hydrogen atoms from the E-map. Full-matrix least-squares/difference Fourier cycles were performed, which located the remaining non-hydrogen atoms. All non-hydrogen atoms were refined with anisotropic displacement parameters (except for $(G3)_1$:$LiBPh_4$, see Supporting Information). All hydrogen atoms were placed in ideal positions and refined as riding atoms with relative isotropic displacement parameters. The program PLATON[23] was used for checking the structures. Additional refinement information is found in the Supporting Information.

Results and Discussion

Single-Crystal Structures of $(G3)_1$:$LiCF_3SO_3$, $(G3)_1$:$LiClO_4$, $(G3)_1$:$LiAsF_6$, and $(G3)_1$:$LiBF_4$. Figure 1 shows the crystal structures of $(G3)_1$:$LiCF_3SO_3$, $(G3)_1$:$LiClO_4$, and $(G3)_1$:$LiAsF_6$, respectively. Crystallographic data for these solvates are reported in Table 1 and selected bond distances and angles are shown in Tables 2−4. The isostructural crystal structure of $(G3)_1$:$LiBF_4$ and the corresponding crystallographic data are reported in the Supporting Information. Despite the differences in anion symmetry and structure, all of the solvates have the same form of structure. Each five-coordinate Li^+ cation is coordinated by four EOs (two each from two different G3 molecules) and one donor atom from a single anion. The G3 molecules are coordinated to two different Li^+ cations, resulting in linear, polymeric chains.

Only one G3$-Li^+$ cation solvate structure has been reported in the Cambridge Crystallography Database[24] to date—a $(G3)_1$:$LiBH_4$ complex isostructural to those with $LiCF_3SO_3$, $LiClO_4$, $LiBF_4$, and $LiAsF_6$, except that each BH_4^- anion is coordinated through two hydrogen donor atoms to a single Li^+ cation.[25] A comparison of the ether O−Li distances indicates similar bond lengths of 1.976(5)−2.250(5), 1.971(11)−2.153(11), and 1.928(13)−2.161(13) Å for $(G3)_1$:$LiCF_3SO_3$, $(G3)_1$:$LiClO_4$, and $(G3)_1$:$LiAsF_6$, respectively. The Cl−O and As−F distances in $(G3)_1$:$LiClO_4$ and $(G3)_1$:$LiAsF_6$, respectively, for the coordinated anion donor atoms are significantly longer than the other Cl−O and As−F distances. This is not observed, however, in the $CF_3SO_3^-$ anions in $(G3)_1$:$LiCF_3SO_3$. The reason for this is unknown.

---

(12) Johansson, P.; Gejji, S. P.; Tegenfeldt, J.; Lindgren, J. *Solid State Ionics* **1996**, *86−88*, 297.

(13) Johansson, P.; Tegenfeldt, J.; Lindgren, J. *J. Phys. Chem. A* **1998**, *102*, 4660.

(14) Sutjianto, A.; Curtiss, L. A. *J. Phys. Chem. A* **1998**, *102*, 968.

(15) Redfern, P. C.; Curtiss, L. A. *J. Power Sources* **2002**, *110*, 401.

(16) Choquette, Y.; Brisard, G.; Parent, M.; Brouillette, D.; Perron, G.; Desnoyers, J. E.; Armand, M.; Gravel, D.; Slougui, N. *J. Electrochem. Soc.* **1998**, *145*, 3500.

(17) Brouillette, D.; Perron, G.; Desnoyers, J. E. *Electrochim. Acta* **1999**, *44*, 4721.

(18) Blessing, R. *Acta Crystallogr. A* **1995**, *51*, 33. Sheldrick, G. M. *SADABS*; Bruker Analytical X-ray Systems: Madison, WI, 2000.

(19) *SAINT V6.1*; Bruker Analytical X-Ray Systems: Madison, WI.

(20) SIR92. Altomare, A.; Cascarano, G.; Giacovazzo, C.; Guagliardi, A. *J. Appl. Crystallogr.* **1993**, *26*, 343.

(21) SIR97. Altomare, A.; Burla, M. C.; Camalli, M.; Cascarano, G.; Giacovazzo, C.; Guagliardi, A.; Moliterni, A. G. G.; Polidori, G.; Spagna, R. *J. Appl. Crystallogr.* **1998**, *32*, 115.

(22) *SHELXTL-Plus V5.10*; Bruker Analytical X-Ray Systems: Madison, WI.

(23) PLATON. Spek, A. L. *Acta Crystallogr. A* **1990**, *46*, C34.

(24) Cambridge Structural Database version 5.21 (April 2001). Allen, F. H.; Kennard, O. *Chem. Des. Automat. News* **1993**, *8*, 3137.

(25) Giese, H.-H.; Nöth, H.; Schwenk, H.; Thomas, S. *Eur. J. Inorg. Chem.* **1998**, 941.

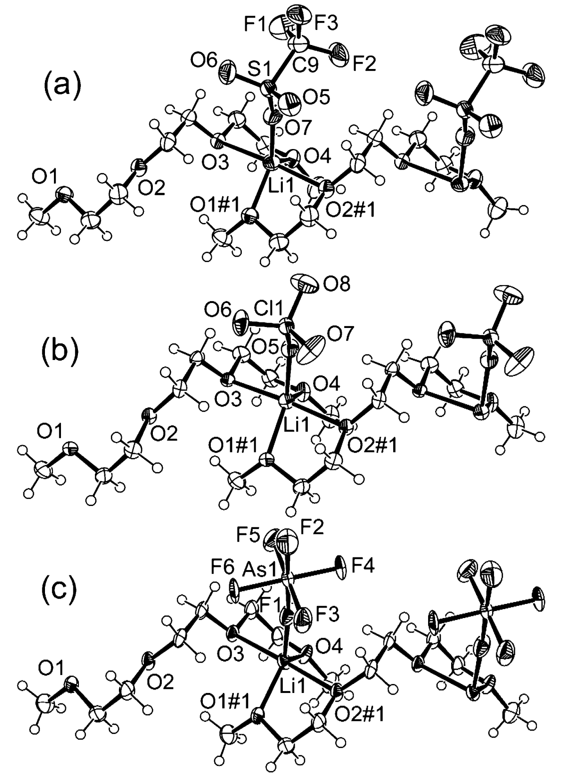

Figure 1. Li$^+$ cation coordination environment in (a) $(G3)_1$:$LiCF_3SO_3$ (anions are disordered over two positions, not shown), (b) $(G3)_1$:$LiClO_4$ (anions are disordered over three positions, not shown), and (c) $(G3)_1$:$LiAsF_6$. Thermal ellipsoids drawn at 50% probability.

Single-Crystal Structure of $(G3)_1$:$LiBPh_4$. Unlike the structures noted above, $LiBPh_4$ forms a new form of $(G3)_1$:LiX complex, $(G3)_1$:$LiBPh_4$, in which the five-coordinate Li$^+$ cations are coordinated solely by the G3 EOs (Figure 2). Crystallographic data for $(G3)_1$:$LiBPh_4$ are reported in the Supporting Information. The G3 molecules adopt a 12-crown-4 (12C4)-like conformation with all four of the EOs coordinating a Li$^+$ cation. One of the EOs, however, uses its second electron lone pair to coordinate a second Li$^+$ cation. Dimeric solvates thus form from two of these in which the cations are each coordinated to EOs from two G3 molecules. A crown ether $[(12C4)Li]_2^{2+}$ solvate with a very similar structure to that of the $[(G3)Li]_2^{2+}$ solvate has been reported.[26] The bulky, noncoordinating BPh_4^- anions in $(G3)_1$:$LiBPh_4$ remain uncoordinated, but six of the anions form a cage around the $[(G3)Li]_2^{2+}$ solvate.

Several $(G3)_1$:NaX structures have been reported.[27−31] These structures differ markedly from those with Li$^+$ cations. The Na$^+$ cations are coordinated by all four G3 EOs, as well as one or two anions. The larger size of the Na$^+$ cations as compared with Li$^+$ cations likely accounts for the differences in coordination between the different solvates.

Ionic Association. The relatively high-donor and low-acceptor numbers of ethers[32] indicates that solvation occurs predominantly through coordination of the cations by the EO electron lone pairs rather than by solvent−anion coordination. Li$^+$ cations in a PEO electrolyte are thus competitively coordinated by both the polymer EOs and neighboring counteranions. Strong cation−anion interactions lead to ionic association into contact ion pair (CIP) or aggregate (AGG) solvate structures when one or more cations are coordinated to an anion, respectively. Therefore, for a given ether solvent and cation, the solvate species present depend on the charge delocalization and coordinating ability of the counteranions as well as the temperature and salt concentration. The following order is found for increasing ionic association of lithium salts in aprotic solvents:[33−37]

$$LiCF_3SO_3 \gg LiBF_4 > LiClO_4 \sim LiI \gg LiAsF_6 > LiBPh_4$$

In glyme-like solvents, $LiAsF_6$ tends to form solvent-separated ion pair (SSIP) solvates in which the cations are fully coordinated by EOs and the anions remain uncoordinated when enough EOs are available for such coordination.[31,33,38] A phase diagram of the $(G3)_n$−$LiAsF_6$ system (not shown) indicates that, in addition to the $(G3)_1$:$LiAsF_6$ phase, a $(G3)_2$:$LiAsF_6$ phase forms. This latter phase is likely to consist of SSIPs perhaps resembling $(G3)_2$:NaX[39−43] and/or $(12C4)_2$:LiX[44,45] solvates. It is therefore noteworthy that, despite the low tendency of AsF_6^- anions to form associated species with solvated Li$^+$ cations and the availability of a SSIP solvate crystal structure (i.e., $(G3)_1$:$LiBPh_4$), the $(G3)_1$:$LiAsF_6$ phase consists of polymeric CIPs. This indicates that the CIP $(G3)_1$:LiX structure is a highly favorable form of Li$^+$ cation coordination. It is important to note, however, that crystal structures resembling these CIP solvates cannot form in PEO electrolytes due to the packing constraints on the long-range ordering of longer polyether chains.

Single-Crystal Structure of $(G3)_{2/3}$:$LiCF_3SO_3$. Crystals of a more concentrated $LiCF_3SO_3$ salt phase, $(G3)_{2/3}$:

---

(26) Dietrich, A.; Neumüller, B.; Dehnicke, K. *Z. Anorg. Allg. Chem.* **1999**, *625*, 619.

(27) Blake, A. J.; Darr, J. A.; Howdle, S. M.; Poliakoff, M.; Li, W.-S.; Webb, P. B. *J. Chem. Crystallogr.* **1999**, *29*, 547.

(28) Bock, H.; Arad, C.; Näther, C.; Havlas, Z. *Helv. Chim. Acta* **1997**, *80*, 606.

(29) Binder, H.; Loos, H.; Borrmann, H.; Simon, A.; Flad, H. J.; Savin, A. *Z. Anorg. Allg. Chem.* **1993**, *619*, 1353.

(30) Linti, G.; Kostler, W. *Chem. Eur. J.* **1998**, *4*, 942.

(31) Rhodes, C. P. Ph.D. Thesis, The University of Oklahoma, Norman, OK, 2001.

(32) Gutmann, V.; Resch, G.; Linert, W. *Coord. Chem. Rev.* **1982**, *43*, 133.

(33) Henderson, W. A. Ph.D. Thesis, University of Minnesota, Minneapolis, MN, 2002.

(34) Ue, M. *J. Electrochem. Soc.* **1994**, *141*, 3336.

(35) Ue, M.; Mori, S. *J. Electrochem. Soc.* **1995**, *142*, 2577.

(36) Ue, M.; Mori, S. In *Rechargeable Lithium and Lithium-Ion Batteries*; Megahead, S., Barnett, B. M., Xie, L., Eds.; The Electrochemical Society Proceedings Series, PV 94-28; The Electrochemical Society: Pennington, NJ, 1995.

(37) Barthel, J.; Gores, H. J. In *Handbook of Battery Materials*; Besenhard, J. O., Ed.; Wiley-VCH: New York, 1999.

(38) MacGlashan, G. S.; Andreev, Y. G.; Bruce, P. G. *Nature* **1999**, *398*, 792.

(39) Bock, H.; Näther, C.; Havlas, Z.; John, A.; Arad, C. *Angew. Chem., Int. Ed. Engl.* **1994**, *33*, 875.

(40) Näther, C.; Bock, H.; Havlas, Z.; Hauck, T. *Organometallics* **1998**, *17*, 4707.

(41) Noordik, J. H.; Beurskens, P. T.; van den Hark, T. E. M.; Smits, J. M. M. *Acta Crystallogr. B* **1979**, *35*, 621.

(42) Bock, H.; Sievert, M.; Bogdan, C. L.; Kolbesen, B. O.; Wittershagen, A. *Organometallics* **1999**, *18*, 2387.

(43) Bock, H.; Hauck, T.; Näther, C.; Havlas, Z. *Z. Naturforsch., B: Chem. Sci.* **1997**, *52*, 524.

(44) Dillon, R. E. A.; Stern, C. L.; Shriver, D. F. *Solid State Ionics* **2000**, *133*, 247.

(45) Olmstead, M. M.; Power, P. P. *J. Am. Chem. Soc.* **1985**, *107*, 2174.

Table 1. Crystal and Refinement Data

structure	$(G3)_1$:$LiCF_3SO_3$	$(G3)_1$:$LiClO_4$	$(G3)_1$:$LiAsF_6$	$(G3)_{2/3}$:$LiCF_3SO_3$
chemical formula	$C_9H_{18}LiF_3O_7S$	$C_8H_{18}LiO_8Cl$	$C_8H_{18}LiF_6O_4As$	$C_{38}H_{72}Li_6F_{18}O_{34}S_6$
fw	334.23	284.61	374.08	1648.96
crystal system	monoclinic	monoclinic	monoclinic	triclinic
space group	$P2_1/c$	$P2_1/c$	$P2_1/n$	P-1
a (Å)	13.017(2)	12.319(3)	6.197(1)	13.1295(16)
b (Å)	6.3311(9)	6.1696(14)	12.697(2)	16.509(2)
c (Å)	18.692(3)	17.285(4)	18.542(3)	19.413(2)
α (deg)	90	90	90	104.573(2)
β (deg)	97.281(2)	94.140(4)	95.458(3)	100.633(2)
γ (deg)	90	90	90	111.656(2)
V (Å^3)	1528.0(4)	1310.3(5)	1452.3(4)	3600.6(7)
Z	4	4	4	2
T (K)	173(2)	173(2)	173(2)	173(2)
ρ_{calc} (g cm^{-3})	1.453	1.443	1.711]	1.521
μ (mm^{-1})	0.270	0.319	2.414	0.318
crystal size (mm)	0.36 × 0.26 × 0.26	0.41 × 0.32 × 0.27	0.32 × 0.14 × 0.13	0.38 × 0.32 × 0.20
F(000)	696	600	752	1696
$2\theta_{max}$ (deg)	27.48	25.17	25.07	25.07
N (R_{int})	3480 (0.028)	2308 (0.0587)	2572 (0.0783)	12665 (0.038)
N [$I > 2\sigma(I)$]	2823	1591	2049	10219
R1,[a] wR2[b] [$I > 2\sigma(I)$]	0.0549, 0.1412	0.0733, 0.1997	0.0704, 0.1846	0.0454, 0.1211
R1,[a] wR2[b] (all data)	0.0680, 0.1464	0.1059, 0.2130	0.0875, 0.1955	0.0573, 0.1337
GOF[c]	1.113	1.139	1.023	1.029
$\Delta e_{min,max}$ (e Å^{-3})	−0.334, 0.436	−0.469, 0.645	−1.650, 1.323	−0.399, 0.523

[a] $R1 = \sum||F_o| - |F_c||/\sum|F_o|$. [b] $wR2 = [\sum[w(F_o^2 - F_c^2)^2]/\sum[w(F_o^2)^2]]^{1/2}$. [c] $GOF = [\sum[w(F_o^2 - F_c^2)^2]/(n - p)]^{1/2}$.

Table 2. Selected Bond Lengths (Å) and Angles (deg) for $(G3)_1$:$LiCF_3SO_3$

Li1−O1#1[a]	1.986(4)	S1−O6	1.431(2)
Li1−O2#1	2.203(5)	S1−O7	1.428(2)
Li1−O3	2.250(5)	S1−C9	1.818(4)
Li1−O4	1.976(5)	C9−F1	1.321(5)
Li1−O7	1.925(4)	C9−F2	1.362(5)
S1−O5	1.428(3)	C9−F3	1.342(4)
O1#1−Li1−O2#1	80.53(16)	O2#1−Li1−O4	96.51(19)
O1#1−Li1−O3	96.94(19)	O2#1−Li1−O7	93.45(19)
O1#1−Li1−O4	115.1(2)	O3−Li1−O4	79.61(16)
O1#1−Li1−O7	125.6(2)	O3−Li1−O7	92.42(18)
O2#1−Li1−O3	174.0(2)	O4−Li1−O7	119.2(2)

[a] Symmetry transformation: (#1) x, $y - 1$, z.

Table 3. Selected Bond Lengths (Å) and Angles (deg) for $(G3)_1$:$LiClO_4$

Li1−O1#1[a]	2.000(10)	Cl1−O5	1.458(5)
Li1−O2#1	2.153(11)	Cl1−O6	1.423(6)
Li1−O3	2.145(11)	Cl1−O7	1.427(6)
Li1−O4	1.971(11)	Cl1−O8	1.417(6)
Li1−O5	2.000(10)		
O1#1−Li1−O2#1	80.9(4)	O2#1−Li1−O4	97.4(5)
O1#1−Li1−O3	95.8(4)	O2#1−Li1−O5	94.1(5)
O1#1−Li1−O4	116.4(5)	O3−Li1−O4	81.7(4)
O1#1−Li1−O5	128.8(6)	O3−Li1−O5	89.9(5)
O2#1−Li1−O3	175.9(5)	O4−Li1−O5	114.7(5)

[a] Symmetry transformation: (#1) x, $y + 1$, z.

Table 4. Selected Bond Lengths (Å) and Angles (deg) for $(G3)_1$:$LiAsF_6$

Li1−O1#1[a]	2.001(13)	As1−F1	1.740(4)
Li1−O2#1	2.161(13)	As1−F2	1.702(5)
Li1−O3	2.124(13)	As1−F3	1.705(5)
Li1−O4	1.928(13)	As1−F4	1.710(4)
Li1−F1	1.994(12)	As1−F5	1.709(5)
		As1−F6	1.710(4)
O1#1−Li1−O2#1	80.6(5)	O2#1−Li1−O4	99.0(5)
O1#1−Li1−O3	97.6(5)	O2#1−Li1−F1	90.3(5)
O1#1−Li1−O4	118.3(6)	O3−Li1−O4	82.3(5)
O1#1−Li1−F1	121.9(6)	O3−Li1−F1	90.1(5)
O2#1−Li1−O3	178.1(7)	O4−Li1−F1	119.8(6)

[a] Symmetry transformation: (#1) $x - 1$, y, z.

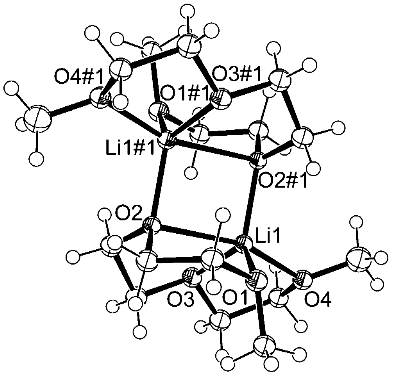

Figure 2. Li^+ cation coordination environment in $(G3)_1$:$LiBPh_4$. The BPh_4^- anions are not shown. Thermal ellipsoids drawn at 50% probability.

$LiCF_3SO_3$, were also prepared and characterized. The Li^+ cation coordination in the asymmetric unit is shown in Figure 3. Crystallographic data for $(G3)_{2/3}$:$LiCF_3SO_3$ are reported in Table 1 and selected bond distances and angles are shown in Table 5. Polymeric chains form between the cations and anions, but two separate forms of cation coordination sites exist. In the first site (i.e., Li1, Li2, Li4, and Li5), the five-coordinate Li^+ cations are coordinated by three EOs (from a single G3 molecule, Figure 4a) and two anion oxygen atoms (one each from two anions). The fourth EO of the G3 molecule is coordinated to another cation. The second site (i.e., Li3 and Li6) consists of four-coordinate Li^+ cations coordinated by two of the G3 end EOs and two anion oxygen atoms (one each from two anions, Figure 4b). These four-coordinate Li^+ cations may also be weakly coordinated by two additional EO electron lone pairs. For example, both O7 and O11 have their uncoordinated lone pairs directed toward Li3 (Li3−O7 and Li3−O11 distances are 2.81 and 3.13 Å, respectively). Note that the EOs (O3, O7, O11, and O15), which may have weak coordination (long O−Li distances) to the latter cations, are also rather weakly coordinated to the former cations with O−Li distances of 2.229(4)−2.492(4) Å. Each of the $CF_3SO_3^-$ anions is coordinated to two Li^+ cations.

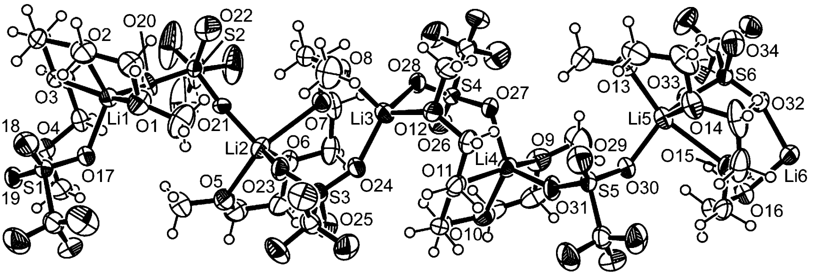

Figure 3. Asymmetric unit of $(G3)_{2/3}$:$LiCF_3SO_3$. Thermal ellipsoids drawn at 50% probability.

Table 5. Selected Bond Lengths (Å) and Angles (deg) for $(G3)_{2/3}$:$LiCF_3SO_3$

Li1−O1	2.087(4)	Li4−O9	2.105(4)
Li1−O2	1.994(4)	Li4−O10	2.000(4)
Li1−O3	2.292(4)	Li4−O11	2.229(4)
Li1−O17	1.962(4)	Li4−O27	1.976(4)
Li1−O20	1.866(13)	Li4−O31	1.902(4)
Li2−O5	2.101(5)	Li5−O13	2.064(4)
Li2−O6	1.988(4)	Li5−O14	1.971(4)
Li2−O7	2.436(4)	Li5−O15	2.492(4)
Li2−O21	1.815(14)	Li5−O30	1.923(4)
Li2−O23	1.941(5)	Li5−O33	1.959(4)
Li3−O8	2.007(4)	Li6−O16	2.022(4)
Li3−O12	2.042(4)	Li6−O4#1^a	2.019(4)
Li3−O24	1.928(6)	Li6−O32	1.933(4)
Li3−O28	1.973(4)	Li6−O19#1	1.990(4)
O1−Li1−O2	80.10(15)	O9−Li4−O10	80.16(16)
O1−Li1−O3	156.0(2)	O9−Li4−O11	155.5(2)
O1−Li1−O17	97.09(18)	O9−Li4−O27	95.13(18)
O1−Li1−O20	108.0(7)	O9−Li4−O31	101.54(19)
O2−Li1−O3	78.05(14)	O10−Li4−O11	79.01(15)
O2−Li1−O17	125.5(2)	O10−Li4−O27	132.5(2)
O2−Li1−O20	116.6(6)	O10−Li4−O31	107.81(19)
O3−Li1−O17	87.69(15)	O11−Li4−O27	89.58(16)
O3−Li1−O20	90.7(7)	O11−Li4−O31	96.93(18)
O17−Li1−O20	115.8(5)	O27−Li4−O31	119.3(2)
O5−Li2−O6	80.32(16)	O13−Li5−O14	81.35(17)
O5−Li2−O7	154.9(2)	O13−Li5−O15	155.2(2)
O5−Li2−O21	100.9(6)	O13−Li5−O30	107.75(19)
O5−Li2−O23	99.2(3)	O13−Li5−O33	100.9(2)
O6−Li2−O7	75.47(15)	O14−Li5−O15	75.00(15)
O6−Li2−O21	115.8(9)	O14−Li5−O30	115.1(2)
O6−Li2−O23	122.6(2)	O14−Li5−O33	123.3(2)
O7−Li2−O21	95.5(6)	O15−Li5−O30	89.32(17)
O7−Li2−O23	88.4(2)	O15−Li5−O33	86.11(16)
O21−Li2−O23	120.5(9)	O30−Li5−O33	117.6(2)
O8−Li3−O12	103.67(19)	O4#1−Li6−O16	99.11(19)
O8−Li3−O24	102.3(2)	O4#1−Li6−O19#1	95.56(17)
O8−Li3−O28	106.12(19)	O4#1−Li6−O32	104.28(19)
O12−Li3−O24	103.0(3)	O16−Li6−O19#1	107.45(19)
O12−Li3−O28	95.27(17)	O16−Li6−O32	98.61(18)
O24−Li3−O28	141.3(3)	O19#1−Li6−O32	144.2(2)

^{a} Symmetry transformation: (#1) $x + 1, y, z - 1$.

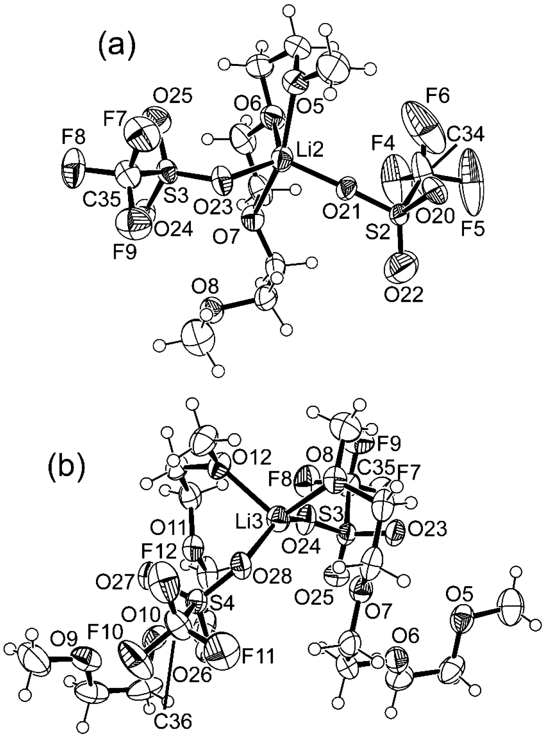

Figure 4. Li$^+$ cation coordination environment of (a) Li2 and (b) Li3 in $(G3)_{2/3}$:$LiCF_3SO_3$. Thermal ellipsoids drawn at 50% probability.

In addition to the reported structures of $(G3)_1$:$LiCF_3SO_3$ and $(G3)_{2/3}$:$LiCF_3SO_3$, a crystal structure for a $(G3)_{1/2}$:$LiCF_3SO_3$ phase is known.[31] This structure strongly resembles a diglyme $(G2)_{1/2}$:$LiCF_3SO_3$ phase.[46] Two separate cation coordination sites exist. In the first site, five-coordinate Li$^+$ cations are again coordinated by three EOs (from a single G3 molecule) and two anion oxygen atoms (one each from two anions) while the second site consists of four-coordinate Li$^+$ cations coordinated by oxygen atoms from four anions and hence not coordinated by the G3 molecules. Each oxygen donor atom of the $CF_3SO_3^-$ anions is coordinated to a separate Li$^+$ cation. Each anion thus coordinates three Li$^+$ cations. The principle difference between the $(G3)_{1/2}$:$LiCF_3SO_3$ and $(G2)_{1/2}$:$LiCF_3SO_3$ structures is a single uncoordinated G3 EO in the former. A comparison of the $(G3)_n$:$LiCF_3SO_3$ solvates structures shows a trend in which the $CF_3SO_3^-$ anions coordinate one ($(G3)_1$:$LiCF_3SO_3$, CIP), two ($(G3)_{2/3}$:$LiCF_3SO_3$, AGG-I), or three ($(G3)_{1/2}$:$LiCF_3SO_3$, AGG-II)[31] Li$^+$ cations, respectively, as the ratio of G3/Li decreases. The AGG-I and AGG-II species refer to $CF_3SO_3^-$ anions coordinated to two or three different Li$^+$ cations, respectively.[47]

Raman spectroscopy of $(G3)_n$−$LiCF_3SO_3$ mixtures indicates that at 25 °C the ratio of SSIP:CIP:AGG-I:AGG-II species are for $n = 20$ (16:78:7:0), $n = 5$ (19:66:15:0), and $n = 1.25$ (8:57:35:0).[48] CIP solvates predominate in dilute mixtures in agreement with the formation of the CIP $(G3)_1$:$LiCF_3SO_3$ crystalline solvate. When the ratio of G3/$LiCF_3SO_3$ approaches 1/1, but the mixture is still amorphous (crystallization of the $(G3)_1$:$LiCF_3SO_3$ phase is slow at 25 °C), a significant fraction of AGG-I species are present, which may resemble the AGG-I $(G3)_{2/3}$:$LiCF_3SO_3$ crystalline solvate. No AGG-II

---

(46) Henderson, W. A.; Young, V. G., Jr.; Brooks, N. R.; Smyrl, W. H. *Acta Crystallogr. C* **2002**, *58*, m501.

(47) Huang, W.; Frech, R.; Wheeler, R. A. *J. Phys. Chem.* **1994**, *98*, 100.

(48) Huang, W.; Frech, R. *Polymer* **1994**, *35*, 235.

species are present, which suggests that the coordination of the anions to three cations does not occur until higher concentrations (i.e., $(G3)_n$-$LiCF_3SO_3$ with $n < 1$) or perhaps at higher temperatures. Measurements of a $n = 5$ mixture between −40 and 25 °C also indicate that CIP solvates are the preferred species, although a significant fraction (∼25%) of SSIP solvates are present at low temperatures. These SSIP solvates may consist of Li^+ cations coordinated to two G3 ligands in the amorphous phase at low temperatures. As the temperature increases, the fraction of SSIP solvates decreases and the CIP and AGG-I solvates increase.[49]

Li^+ Cation Transport Mechanisms in Associated PEO Electrolytes. In PEO electrolytes containing associated salts (e.g., $LiCF_3SO_3$), the solvated cations typically exist as CIP and/or AGG solvates, even for relatively dilute concentrations.[50,51] The AGG solvates are likely to be coordinated by a single PEO chain (three EOs) and two anions. This form of Li^+ cation solvate is highly favorable, as evidenced by the Li^+ cation coordination in $(G3)_{2/3}$:$LiCF_3SO_3$, $(G3)_{1/2}$:$LiCF_3SO_3$,[31] $(G2)_1$:$LiCF_3SO_3$,[52] $(G2)_{1/2}$:$LiCF_3SO_3$,[42] and $P(EO)_3$:$LiCF_3SO_3$.[53]

Note that there is no direct interaction between the neighboring chains in the $P(EO)_3$:$LiCF_3SO_3$ crystal structure. Macroscopic cationic transport, however, requires that the cations move between polyether chains. It is unclear how associated cations coordinated by a single polymer chain become coordinated by a new chain. Molecular modeling of $P(EO)_n$−LiI systems has suggested that while movement of an associated Li^+ cation along a single chain may occur readily, the transfer to another chain is a relatively rare event.[54−56] The cations appear to move back and forth along a single chain numerous times before a suitable transition state solvate conformation occurs that enables them to move to a new chain. A high Li^+ cation coordination, either by EOs and/or anions, reduces the energy barriers of such transition states.[57,58] The validity of the molecular models, however, should be verified experimentally whenever possible. The solvate structures reported here offer one means of doing so.

The Li^+ cation coordination in the CIP structures of $(G3)_1$:$LiCF_3SO_3$, $(G3)_1$:$LiClO_4$, $(G3)_1$:$LiAsF_6$, and $(G3)_1$:$LiBF_4$ suggests one mechanism for associated Li^+ cation transport between polymer chains. In the amorphous phase, the encroachment of a second polymer chain upon a cation coordinated by a single polymer chain and one or more anions may permit a two-chain CIP solvate to form similar to $(G3)_1$:$LiCF_3SO_3$, $(G3)_1$:$LiClO_4$, $(G3)_1$:$LiAsF_6$, and $(G3)_1$:$LiBF_4$. When this solvate breaks apart, the cation may be transferred to the new polymer chain (or back to the original chain). Alternatively, a two-chain AGG solvate may form similar to the Li^+ cation coordination found in $(G3)_{2/3}$:$LiCF_3SO_3$, leading to a different interchain cationic transport mechanism. In each anion-assisted mechanism (interchain solvate transition state), the cation coordination remains high (4- or 5-fold). The utility of exploring glyme−salt solvate structures becomes evident when one notes that both types of Li^+ cation transport mechanisms have been reported from molecular modeling studies.[54]

Acknowledgment. W.A.H. is indebted to the National Science Foundation for the award of a NSF Graduate Research Fellowship and the University of Minnesota for a Graduate Research Fellowship.

Supporting Information Available: X-ray crystallographic data files (CIFs) for $(G3)_1$:$LiCF_3SO_3$, $(G3)_1$:$LiClO_4$, $(G3)_1$:$LiAsF_6$, and $(G3)_{2/3}$:$LiCF_3SO_3$. X-ray crystallographic data for $(G3)_1$:$LiBF_4$ and $(G3)_1$:$LiBPh_4$. Structure refinement and additional drawings for the solvate structures (pdf). This material is available free of charge via the Internet at http://pubs.acs.org.

CM034351Z

---

(49) Frech, R.; Huang, W. *Solid State Ionics* **1994**, *72*, 103.

(50) Brodin, A.; Mattson, B.; Nilsson, K.; Torell, L. M.; Hamara, J. *Solid State Ionics* **1996**, *85*, 111.

(51) Chintapalli, S.; Frech, R. *Electrochim. Acta* **1998**, *43*, 1395.

(52) Rhodes, C. P.; Frech, R. *Macromolecules* **2001**, *34*, 2660.

(53) Lightfoot, P.; Mehta, M. A.; Bruce, P. G. *Science* **1993**, *262*, 883.

(54) Müller-Plathe, F.; van Gunsteren, W. F. *J. Chem. Phys.* **1995**, *103*, 4745.

(55) Borodin, O.; Smith, G. D. *J. Phys. Chem. B* **2000**, *104*, 8017.

(56) Borodin, O.; Smith, G. D. *Macromolecules* **2000**, *33*, 2273.

(57) Baboul, A. G.; Redfern, P. C.; Sutjianto, A.; Curtiss, L. A. *J. Am. Chem. Soc.* **1999**, *121*, 7220.

(58) Sutjianto, A.; Curtiss, L. A. *J. Phys. Chem. A* **1998**, *102*, 968.